

1 **Characteristics and mixing state of amine-containing**
2 **particles at a rural site in the Pearl River Delta, China.**

3
4 Chunlei Cheng^{1,2}, Zuzhao Huang³, Chak K. Chan⁴, Yangxi Chu⁴, Mei Li^{1,2*}, Tao
5 Zhang⁵, Yubo Ou⁵, Duohong Chen⁵, Peng Cheng^{1,2}, Lei Li^{1,2}, Wei Gao^{1,2}, Zhengxu
6 Huang^{1,2}, Bo Huang^{1,2,6}, Zhong Fu⁶, Zhen Zhou^{1,2*}

7
8 ¹Institute of Mass Spectrometer and Atmospheric Environment, Jinan University, Guangzhou 510632,
9 China

10 ²Guangdong Provincial Engineering Research Center for on-line source apportionment system of air po
11 llution, Guangzhou 510632, China

12 ³Guangzhou Environmental Technology Assessment Center, Guangzhou 510045, China

13 ⁴School of Energy and Environment, City University of Hong Kong, Hong Kong, China

14 ⁵State Environmental Protection Key Laboratory of Regional Air Quality Monitoring, Guangdong
15 Environmental Monitoring Center, Guangzhou 510308, China

16 ⁶Guangzhou Hexin Analytical Instrument Limited Company, Guangzhou 510530, China

17
18
19 **Correspondence to:* Mei Li (limei2007@163.com) and Zhen Zhou (zhouzhen@gig.ac.cn)

20 Tel: 86-20-85225991, Fax: 86-20-85225991

43 **Abstract.** Particulate amines play an important role for the particle acidity and
44 hygroscopicity and also contribute to secondary organic aerosol mass. We investigated
45 the sources and mixing states of particulate amines using a single-particle aerosol
46 mass spectrometer (SPAMS) during summer and winter 2014 at a rural site in the
47 Pearl River Delta, China. Amine-containing particles accounted for 11.1 % and 9.4 %
48 of the total detected individual particles in summer and winter, respectively. Although
49 the increase of amine-containing particle counts mostly occurred at night, no obvious
50 correlations between amine-containing particles and ambient relative humidity (RH)
51 were found during the sampling period. Among the three markers we considered, the
52 most abundant amine marker was $^{74}(\text{C}_2\text{H}_5)_2\text{NH}_2^+$, which was detected in 90% and 86%
53 of amine-containing particles in summer and winter, followed by amine marker ions
54 of $^{59}(\text{CH}_3)_3\text{N}^+$, and $^{86}(\text{C}_2\text{H}_5)_2\text{NCH}_2^+$ which were detected in less than 10% of
55 amine-containing particles during sampling period. The amine-containing particles
56 were characterized by high fractions of carbonaceous marker ions, carbon-nitrogen
57 fragments, sulfate and nitrate in both summer and winter. More than 90% of
58 amine-containing particles were found to be internally mixed with sulfate throughout
59 the sampling period, while the percentage of amine particles containing nitrate
60 increased from 43% in summer to 69% in winter. Robust correlations between the
61 peak intensities of amines and sulfate and nitrate were observed, suggesting the
62 possible formation of aminium sulfate and nitrate salts. Interestingly, only 8% of
63 amine particles contained ammonium in summer, while the percentage increased
64 dramatically to 54 % in winter, indicating a relatively ammonium-poor state in
65 summer and an ammonium-rich state in winter. The total ammonium-containing
66 particles were investigated and showed a much lower abundance in ambient particles
67 in summer (3.6%) than that in winter (32.6%), which suggests the ammonium-poor
68 state of amine-containing particles in summer may be related to the lower abundance
69 of ammonia/ammonium in gas and particle phase. In addition, higher abundance of
70 amines in ammonium-containing particles than that of ammonium in
71 amine-containing particles suggests a possible contribution of ammonium–amine
72 exchange reactions to the low abundance of ammonium in amine-containing particles

73 at high ambient RH (72 ± 13 %) in summer. The particle acidity of amine-containing
74 particles is estimated via the relative acidity ratio (R_a), which is defined as the ratio of
75 the sum of the sulfate and nitrate peak areas divided by the ammonium peak area. The
76 R_a was 326 ± 326 in summer and 31 ± 13 in winter, indicating that the
77 amine-containing particles were more acidic in summer than in winter. However, after
78 including amines along with the ammonium in the acidity calculation, the new R_a'
79 values showed no seasonal change in summer (11 ± 4) and winter (10 ± 2), which
80 suggests that amines could be a buffer for the particle acidity of ammonium-poor
81 particles.

82 **Keywords:** Amine; Single particles; Mixing state; Ammonium salts; Particle acidity;
83 SPAMS.

84 **1 Introduction**

85 Amines, a group of nitrogen-containing organic compounds, are ubiquitous in
86 the atmospheric gas and particle phases (Ge et al., 2011a). A variety of low molecular
87 weight (LMW) aliphatic amines have been detected in emissions from anthropogenic
88 and natural sources, including animal husbandry, biomass burning, industrial
89 emissions, vehicle exhaust, and marine sources (Rogge et al., 1994; Rappert and
90 Muller, 2005; Calderon et al., 2007; Ngwabie et al., 2007; Facchini et al., 2008; Ge et al.,
91 2011a). LMW aliphatic amines have gas-phase concentrations two orders of
92 magnitude lower than that of ammonia (NH_3) (Sorooshian et al., 2008), but are more
93 alkaline than NH_3 (Ge et al., 2011b). Due to their strong basicity and water solubility,
94 LMW amines can undergo acid-base reactions with sulfuric and nitric acid to form
95 ammonium salts (Angelino et al., 2001; Sorooshian et al., 2007; Pratt et al., 2009), which
96 has been found to enhance new particle formation beyond the amounts produced from
97 reactions between acids and NH_3 alone (Kurten et al., 2008; Berndt et al., 2010; Place
98 et al., 2010; Wang et al., 2010). In addition, once partitioned into the particle phase,
99 these LMW aliphatic amines can enhance aerosol particle hygroscopicity (Chu et al.,
100 2015; Sauerwein et al., 2015). Furthermore, amines can be oxidized by OH radicals,
101 NO_3 radicals, and O_3 in the atmosphere to form semi-volatile and non-volatile

102 compounds, some of which are highly toxic (Lee and Wexler, 2013), and which
103 contribute to secondary organic aerosol (SOA) mass (Murphy et al., 2007;Malloy et
104 al., 2009).

105 The mass concentration and temporal distribution of LMW aliphatic amines in
106 aerosols have been studied extensively in a variety of environments, and LMW
107 aliphatic amines account for 2–12 % of organic mass (Day et al., 2009;Gilardoni et al.,
108 2009;Liu et al., 2009;Russell et al., 2009;Williams et al., 2010). In recent years,
109 real-time single particle mass spectrometry has been used to measure the size and
110 chemical composition of individual amine-containing particles with high time
111 resolution. The mixing state and single-particle characteristics of amines have been
112 investigated in laboratory and field environments (Angelino et al., 2001;Moffet et al.,
113 2008;Silva et al., 2008;Pratt et al., 2009;Huang et al., 2012;Qin et al., 2012;Zhang et
114 al., 2012;Gaston et al., 2013;Zauscher et al., 2013). Pratt et al. (2009) studied seasonal
115 differences in aminium and ammonium salts on a single-particle basis using an
116 aerosol time-of-flight mass spectrometer (ATOFMS) coupled with a thermodenuder
117 and reported that the gas-to-particle partitioning of amines is dependent on particle
118 acidity. Healy et al. (2015) investigated the temporal distributions of alkylamines at
119 five European sites, and found that alkylamines were internally mixed with both
120 sulfate and nitrate, which suggests that the formation of aminium salts was important
121 at all sites. Zauscher et al. (2013) detected strong signals of amine marker
122 ($^{86}(\text{C}_2\text{H}_5)_2\text{NCH}_2^+$) in biomass burning aerosols associated with the increase of ambient
123 relative humidity, indicating the direct emission of amines from biomass burning and
124 the important influence of high RH (>90%) on the partitioning process of amines.
125 Huang et al. (2012) determined the mixing state of amine-containing particles in
126 Shanghai and found higher number concentrations of amine-containing particles in
127 winter than in summer, which they attributed to effective acid-base reactions between
128 sulfuric acid and amines under low-temperature, high-RH conditions. Zhang et al.
129 (2012) measured trimethylamine-containing particles in Guangzhou and found
130 preferential trimethylamine gas-to-particle partitioning during fog events. These field
131 observations emphasize the important role of acid-base reactions in the partitioning of

132 amines from the gas phase to the particle phase. Recent laboratory studies have
133 revealed that the exchange between amine gases and particulate NH_3 and/or
134 ammonium also contributes substantially to amine content and results in a depletion
135 of NH_3 and/or ammonium in the particle phase (Lloyd et al., 2009;Bzdek et al.,
136 2010;Qiu et al., 2011;Liu et al., 2012;Chan and Chan, 2013;Chu and Chan, 2016,
137 2017;Sauerwein and Chan, 2017); however, the significance of such exchange
138 reactions in the ambient environment has not been fully explored. Therefore, the
139 influence of ammonia and particle acidity on the distribution of amines in the particle
140 phase should be studied comprehensively through field measurements.

141 The aim of this study was to investigate the mixing state of a series of LMW
142 aliphatic amines with sulfate, nitrate, and ammonium in individual particles using a
143 single-particle aerosol mass spectrometer (SPAMS) at a rural site in the Pearl River
144 Delta, China. In order to explore amine origins and gas-to-particle partitioning
145 processes, amine-containing particles from both summer and winter were classified
146 into three types based on mass spectral patterns. The ammonium sulfate and nitrate salt
147 formation processes and internal mixing state with ammonium were used to deduce
148 the relationship between amines and ammonium in the particle phase and the
149 influence of amines on particle acidity.

150 **2 Methods**

151 **2.1 Aerosol sampling**

152 Ambient single particles were collected and analyzed using a SPAMS at the
153 Guangdong Atmospheric Supersite (22.73° N, 112.93° E), a rural site in Heshan City
154 in the Pearl River Delta (PRD), China (Figure S1). The sampling site is surrounded by
155 villages and experiences little influence from local industrial emissions (Cheng et al.,
156 2017). The SPAMS was installed at the top of the main building, and aerosols were
157 introduced to the SPAMS through a 2.5 m copper tube and a silica gel drier. SPAMS
158 sampling was conducted continuously from 18 July to 1 August 2014 and from 27
159 January to 8 February 2015; several hours of data are missing due to technical
160 maintenance. During the sampling period, hourly O_3 concentrations were measured

161 using an O₃ analyzer (model 49i, Thermo Scientific). Meteorological data, including
162 temperature, relative humidity, wind speed, and wind direction, were also measured
163 during SPAMS sampling.

164 **2.2 SPAMS**

165 SPAMS was designed by the Guangzhou Hexin Analytical Company based on
166 preexisting ATOFMS principles (Prather et al., 1994; Noble and Prather, 1996). The
167 setup and design of the SPAMS has been detailed previously (Li et al., 2011). Briefly,
168 single particles are sampled through an 80 μm critical orifice into the aerodynamic
169 lens at a flow rate of 75 ml min⁻¹. Then, the particles pass consecutively through two
170 laser beams (diode Nd:YAG, 532 nm) spaced 6 cm apart, and the aerodynamic
171 diameter of the single particle is calculated using the particle flight time and velocity
172 between the two laser beams. The single particle velocity is also used to calculate the
173 precise time at which to fire the desorption and ionization laser (Nd:YAG laser,
174 266nm), which is positioned 12 cm downstream from the second laser beam. After
175 ionization, the positive and negative ions are detected by a Z-shaped bipolar
176 time-of-flight mass spectrometer. In this work, the ionization laser pulse energy was
177 0.6 mJ and the power density was 1.06×10^8 W cm⁻² throughout the campaign. The
178 size range of single particles detected by SPAMS ranged from 0.2 to 2 μm, calibrated
179 with standard polystyrene latex spheres (Nanosphere size standards, Duke Scientific
180 Corp., Palo Alto) of 0.22–2.0 μm diameter before and after the campaign (Cheng et al.,
181 2017).

182 **2.3 Data analysis**

183 Particle size and chemical composition were obtained via SPAMS mass spectral
184 analysis using the Computational Continuation Core (COCO; version 3.0) toolkit in
185 Matlab. According to the field studies of ATOFMS and SPAMS, it is difficult to
186 accurately determine the number concentration of ambient particles using SPAMS
187 alone due to the size-dependent transmission efficiencies of particles through
188 aerodynamic lens and composition dependent matrix effect (Gross et al., 2000; Pratt
189 and Prather, 2012). Thus, the particle counts and size distributions presented in this
190 work should be interpreted as semi-quantitative and serve as a basis of comparison

191 analysis (Healy et al., 2012). Based on previous studies using ATOFMS and SPAMS
192 instruments (Angelino et al., 2001;Huang et al., 2012;Qin et al., 2012;Zhang et al.,
193 2012;Gaston et al., 2013;Zauscher et al., 2013;Healy et al., 2015), amine-containing
194 particles were characterized by marker ions, including m/z $^{59}(\text{CH}_3)_3\text{N}^+$, $^{74}(\text{C}_2\text{H}_5)_2\text{NH}_2^+$,
195 $^{86}(\text{C}_2\text{H}_5)_2\text{NCH}_2^+$, $^{101}(\text{C}_2\text{H}_5)_3\text{N}^+$, $^{102}(\text{C}_3\text{H}_7)_2\text{NH}_2^+$, and $^{143}(\text{C}_3\text{H}_7)_3\text{N}^+$ (Table 1). In this
196 work, a particle was identified as amine-containing if it contained any of the marker
197 ions listed above with a relative peak area (defined as the percentage contribution of
198 the target ion peak area to the sum of all ion peak areas) greater than 1%. It should be
199 noted that amine-containing particles are operationally defined and not exclusive,
200 which also contained various chemical species in addition to amines. According to
201 this criterion, 57452 and 68026 amine-containing particles were identified in summer
202 and winter, respectively, which accounted for 11.1 % and 9.4 % of the total detected
203 particles. These number fractions are consistent with previously reported observations
204 in the PRD (Zhang et al., 2012). However, due to the absence of fog events during the
205 campaign, no dramatic increases in amine-containing particles associated with high
206 RH conditions (RH > 90 %) were observed. Marker ions of $^{59}(\text{CH}_3)_3\text{N}^+$,
207 $^{74}(\text{C}_2\text{H}_5)_2\text{NH}_2^+$, $^{86}(\text{C}_2\text{H}_5)_2\text{NCH}_2^+$ were detected as the most abundant amines species
208 during the sampling period, so particles containing each marker ion were selected to
209 investigate the possible sources and characteristics of amine-containing particles.
210 $^{30}\text{CH}_3\text{NH}^+$ is also an amine marker which has been reported by other single particle
211 studies (Phares et al., 2003;Glagolenko and Phares, 2004). In this work the peak
212 intensity of $^{30}\text{CH}_3\text{NH}^+$ was much lower compared with other amine markers, and all
213 the particles containing $^{30}\text{CH}_3\text{NH}^+$ had strong signal of $^{74}(\text{C}_2\text{H}_5)_2\text{NH}_2^+$, so the
214 $^{30}\text{CH}_3\text{NH}^+$ -containing particles were not specifically discussed. An ion peak at m/z
215 +46 was detected in the ambient single particles, which could be the amine marker of
216 $^{46}(\text{CH}_3)_2\text{NH}_2^+$ and/or $^{46}\text{Na}_2^+$ according to reported studies (Guazzotti et al.,
217 2001;Gaston et al., 2011;Healy et al., 2015). In this work the m/z +46-containing
218 particles had no other amine markers as listed above, besides, these particles were
219 enriched with sodium salts like $^{62}\text{Na}_2\text{O}^+$, $^{81}\text{Na}_2\text{Cl}^+$ and $^{147}\text{Na}(\text{NO}_3)_2^-$. Thus, m/z
220 +46-containing particles were not classified as amine-containing particles and are

221 likely sea salts.

222 **3 Results and Discussion**

223 **3.1 Seasonal variation of amine-containing particles**

224 Spatial distributions of amine-containing particles associated with backward
225 trajectories (48 hour) of air masses at 500m levels above the ground during the
226 sampling period are shown in Figure 1. Cluster trajectories were calculated by
227 MeteoInfo (Wang, 2014), and the box plots were conducted by Igor Pro-based
228 program Histbox (Wu et al., 2018;Wu and Yu, 2018). In summer, high
229 amine-containing particle counts were associated with air masses of Cluster 3
230 (41.67%) and Cluster 4 (30.06%) (Figure 1a) from continent and South China Sea
231 separately, suggesting that the majority of amine-containing particles came from
232 anthropogenic sources and coastal emissions. However, in winter, large amounts of
233 amine-containing particles were associated with air masses of Cluster 4 (48.08%)
234 (Figure 1b), indicating that amine-containing particles were related primarily with
235 local emissions, such as animal husbandry, biomass burning, and vehicle exhaust.
236 Anthropogenic emissions from Foshan and Guangzhou may also have contributed, as
237 the sampling site is only 40 km and 56 km from these cities, respectively (Figure S1).
238 Besides, the stagnant meteorological conditions associated with Cluster 4 also
239 facilitated the partitioning of amines from gas to particle phase in winter.

240 The amine-containing particle count observed in summer (57452) was lower than
241 it observed in winter (68026), but the abundance of amine-containing particles
242 relative to the total particle count was higher in summer (11.1%) than in winter (9.4%).
243 Temporal variations of total amine-containing particles and three amine marker ions
244 are shown in Figure 2. The increase of amine-containing particles was mostly
245 associated with high relative humidity (RH) at night in summer, while no direct
246 connection between particle counts and RH was found in winter (Figure S2 a and b).
247 High counts of amine-containing particles that extended in a few days were found
248 from 22 to 24 July (in summer) and from 5 to 8 February (in winter). Among the three
249 markers we considered, the most abundant amine marker was $^{74}(\text{C}_2\text{H}_5)_2\text{NH}_2^+$, which

250 was detected in 90% and 86% of amine-containing particles in summer and winter
251 (Table 2), followed by $^{59}(\text{CH}_3)_3\text{N}^+$ and $^{86}(\text{C}_2\text{H}_5)_2\text{NCH}_2^+$ which were detected in less
252 than 10% of amine-containing particles during sampling period. The amine particles
253 containing $^{74}(\text{C}_2\text{H}_5)_2\text{NH}_2^+$ and $^{86}(\text{C}_2\text{H}_5)_2\text{NCH}_2^+$ both exhibited a similar pattern with
254 total amine-containing particles suggesting a similar emission source of
255 $^{74}(\text{C}_2\text{H}_5)_2\text{NH}_2^+$ and $^{86}(\text{C}_2\text{H}_5)_2\text{NCH}_2^+$ (Figure 2). The temporal trend of
256 $^{59}(\text{CH}_3)_3\text{N}^+$ -containing particles were different from those of $^{74}(\text{C}_2\text{H}_5)_2\text{NH}_2^+$ and
257 $^{86}(\text{C}_2\text{H}_5)_2\text{NCH}_2^+$; and the two sudden episodes of $^{59}(\text{CH}_3)_3\text{N}^+$ occurred from 27 to 29
258 July in summer were possibly due to the emission sources of trimethylamine (TMA).

259 The diurnal patterns of amine-containing particles are investigated in summer
260 and winter (Figure 3) and both showed higher counts at night. The small increase
261 from 6:00 to 9:00 LST throughout the campaign may have been due to local
262 emissions from vehicle exhaust (Cadle and Mulawa, 1980). Several field studies have
263 revealed the strong correlation between RH and particulate amines, suggesting that
264 high RH in fog events is favorable for the gas-to-particle partitioning of amines
265 (Jeong et al., 2011; Rehbein et al., 2011; Huang et al., 2012; Zhang et al., 2012). In this
266 work, although the increase of amine-containing particle counts mostly occurred at
267 night, no obvious correlations between diurnal amine-containing particles and RH
268 were found in summer ($r^2=0.33$) and winter ($r^2=0.0003$) (Figure S2). Although lower
269 temperature facilitates the partitioning of gaseous amines into the particulate phase
270 (Huang et al., 2012), no significant temperature differences were found both in
271 summer (day: 32 ± 1.1 °C; night: 27.5 ± 1.1 °C) and winter (day: 15 ± 1.4 °C; night:
272 13 ± 0.8 °C), which suggests a minor influence of temperature on the diurnal pattern of
273 amine-containing particles. The increase of amine-containing particles at night may be
274 influenced by particle acidity and emission sources of amines (Murphy et al.,
275 2007; Kurten et al., 2008; Silva et al., 2008).

276 3.2 Characteristics of amine-containing particles

277 The average mass spectra of amine-containing particles in summer and winter
278 are shown in Figure 4. The amine-containing particles were characterized by high
279 fractions of carbonaceous marker ions, including $^{27}\text{C}_2\text{H}_3^+$, $^{29}\text{C}_2\text{H}_5^+$, $^{36}\text{C}_3^+$, $^{37}\text{C}_3\text{H}^+$,

280 $^{43}\text{C}_2\text{H}_3\text{O}^+$, $^{48}\text{C}_4^+$, $^{51}\text{C}_4\text{H}_3^+$, $^{53}\text{C}_4\text{H}_5^+$, $^{60}\text{C}_5^+$, $^{63}\text{C}_5\text{H}_3^+$, $^{65}\text{C}_5\text{H}_5^+$, and $^{77}\text{C}_6\text{H}_5^+$; and amine
281 marker ions of $^{30}\text{CH}_3\text{NH}^+$, $^{59}(\text{CH}_3)_3\text{N}^+$, $^{74}(\text{C}_2\text{H}_5)_2\text{NH}_2^+$ and $^{86}(\text{C}_2\text{H}_5)_2\text{NCH}_2^+$ in the
282 positive mass spectrum in both summer and winter. The negative mass spectrum was
283 characterized by strong carbon-nitrogen fragments like $^{26}\text{CN}^-$ and $^{42}\text{CNO}^-$, as well as
284 abundant secondary ions of $^{46}\text{NO}_2^-$, $^{62}\text{NO}_3^-$, $^{80}\text{SO}_3^-$, and $^{97}\text{HSO}_4^-$ in both summer and
285 winter. In many field studies, aged carbonaceous particles always contain abundant
286 secondary ions of sulfate, nitrate, and ammonium. Interestingly, in this work, the
287 signals of $^{18}\text{NH}_4^+$ were weak and only observed in less than 10% of amine-containing
288 particles in summer, but moderate signal of $^{18}\text{NH}_4^+$ was detected in half of
289 amine-containing particles in winter. The low $^{18}\text{NH}_4^+$ signal in amine-containing
290 particles may have been due to the emission sources of ammonia and particle acidity,
291 which will be discussed in Section 3.3.

292 The unscaled size-resolved number distributions of total amine-containing
293 particles and amine particles containing three marker ions of $^{59}(\text{CH}_3)_3\text{N}^+$,
294 $^{74}(\text{C}_2\text{H}_5)_2\text{NH}_2^+$, and $^{86}(\text{C}_2\text{H}_5)_2\text{NCH}_2^+$ are shown in Figure 5. The amine-containing
295 particles exhibited unimodal distributions in the submicron mode from 0.4 to 1.5 μm
296 in both summer and winter, which may have resulted from gaseous amine
297 condensation on and/or reaction with fine mode particles from anthropogenic
298 emissions. Although amine-containing particles peaked at the size range of 0.5-0.7 μm
299 in both summer and winter, a broader size range of amine-containing particles was
300 observed in winter, which may be due to more complex anthropogenic emission
301 sources of primary particles in winter. The $^{74}(\text{C}_2\text{H}_5)_2\text{NH}_2^+$ -containing particles showed
302 similar variation patterns as total amine-containing particles both in summer and
303 winter. However, $^{59}(\text{CH}_3)_3\text{N}^+$ - and $^{86}(\text{C}_2\text{H}_5)_2\text{NCH}_2^+$ -containing particles showed less
304 distinct peaks in winter.

305 **3.3 Mixing state of amine-containing particles**

306 To investigate the mixing state of amine-containing particles, the abundances of
307 sulfate-, nitrate-, and ammonium-containing amine particles are shown in Table 3.
308 More than 90% of amine-containing particles were found to be internally mixed with
309 sulfate throughout the sampling period. The abundance of nitrate in amine particles

310 increased from 43% in summer to 69% in winter. The internal mixing state of amines
311 with sulfate and nitrate had also been found in Qin et al. (2012), which reported that
312 the amine-rich particles consisted of $18 \pm 10\%$ amines by mass in the form of aminium
313 sulfate and nitrate salts in summer in Riverside, California. In this work, the high
314 abundances of sulfate and nitrate in amine-containing particles suggest the possible
315 formation of aminium sulfate and nitrate salts. Interestingly, only 8% of
316 amine-containing particles mixed with ammonium (NH_4^+) in summer, while the
317 percentage increased dramatically to 54 % in winter, indicating a relatively NH_4^+ -poor
318 state in summer and an NH_4^+ -rich state in winter.

319 The seasonal differences of the mixing state of amines and NH_4^+ may be
320 influenced by the seasonal variation of source strength of NH_4^+ . To investigate the
321 temporal variation and abundance of NH_4^+ in total detected single particles, the total
322 NH_4^+ -containing particles were identified with relative area of $^{18}\text{NH}_4^+$ larger than 1%.
323 Using this criterion, 18336 and 235312 of NH_4^+ -containing particles were detected in
324 summer and winter separately, accounting for 3.6% and 32.6% of the total detected
325 particles. The averaged positive and negative ion mass spectra of NH_4^+ -containing
326 particles are exhibited in Figure 6. During the entire sampling period the
327 NH_4^+ -containing particles were characterized by abundant hydrocarbon fragments and
328 secondary organic species like $^{43}\text{C}_2\text{H}_3\text{O}^+$ and $^{89}\text{HC}_2\text{O}_4^-$, as well as strong signals of
329 $^{26}\text{CN}^-$, $^{42}\text{CNO}^-$, $^{62}\text{NO}_3^-$ and $^{97}\text{HSO}_4^-$, indicating an mixing state of NH_4^+ -containing
330 particles. Also, 20% of NH_4^+ -containing particles contained $^{74}(\text{C}_2\text{H}_5)_2\text{NH}_2^+$, which
331 indicates a close connection between NH_3 and diethylamine (DEA), possibly due to
332 the similar emission sources.

333 Temporal variations of total amine-containing particles, total
334 ammonium-containing (NH_4^+ -containing) particles and particles containing both
335 ammonium and amine (NH_4^+ -amine) are shown in Figure 7. The total
336 NH_4^+ -containing particles and NH_4^+ -amine particles were both much lower in summer
337 than in winter, and the NH_4^+ -containing particles and amine-containing particles
338 showed a robust linear correlation in winter ($r^2=0.63$) (Figure S3). This seasonal
339 difference may be due to the low emission sources of ammonia and preferred

340 partitioning in gas phase in summer. Backward trajectories analysis (Figure 1) showed
341 that in summer the air mass was mainly from south of the sampling site and linked to
342 the marine region with low emission of anthropogenic pollutants. By contrast, in
343 winter, the air mass was mainly from northwest of the sampling site and associated
344 with relatively polluted megacities like Guangzhou and Foshan. In this work the lower
345 abundance of NH_4^+ was observed in summer ($\text{RH} = 72 \pm 13\%$) than in winter (RH
346 $=63 \pm 11\%$), suggesting a more important influence of sources than RH on the
347 seasonal trends of NH_4^+ -containing particles.

348 The temporal variations of the peak areas of amines, ammonium, sulfate and
349 nitrate in amine-containing particles are shown in Figure 8. The peak areas of amines
350 and sulfate had similar variation patterns both in summer and winter, and the linear
351 regression between them showed robust correlations both in summer ($r^2=0.69$) and
352 winter ($r^2=0.72$) (Figure S4), indicating the formation of ammonium sulfate salt during
353 the entire sampling period. However, the peak areas of amines and nitrate only
354 exhibited similar trends in winter, and the linear regression between them showed a
355 better correlation in winter ($r^2=0.78$) than in summer ($r^2=0.52$) (Figure S4), suggesting
356 the possible formation of ammonium nitrate salt in winter. Low peak area of ammonium
357 was found in the amine-containing particles in summer which was in accordance with
358 the small amount of NH_4^+ -amine particles. However, in winter, the peak area of
359 ammonium was comparable with amines and they both exhibited similar temporal
360 trends. In this work the particle acidity of amine-containing particles is represented by
361 the relative acidity ratio (R_a), which is developed by Denkenberger et al. (2007) and
362 Pratt et al. (2009), defined as the ratio of the sum of the sulfate and nitrate peak areas
363 divided by the ammonium peak area (Denkenberger et al., 2007;Pratt et al.,
364 2009;Cheng et al., 2017). Huang et al. (2013) obtained a robust correlation ($r^2=0.82$)
365 between the particle acidity calculated from inorganic ions obtained from MARGA
366 and relative acidity ratio obtained from single particle mass spectrometer, allowing us
367 to use R_a for comparison of particle acidity(Huang et al., 2013). The R_a was 326 ± 326
368 in summer and 31 ± 13 in winter (Figure 8), indicating that the amine-containing
369 particles were more acidic in summer than in winter.

370 Although high acidity promotes gaseous ammonia partitioning, extremely low
371 ammonium peak areas were found for the amine-containing particles in summer
372 (Figure 8), which may be associated with ammonium–amine exchange reactions in
373 addition to the low emission source of ammonia. The exchange between amine gases
374 and particulate NH_3 and/or ammonium highly depends on the RH and particle acidity
375 (Chan and Chan, 2013; Chu and Chan, 2016). According to the study of Sauerwein
376 and Chan, the co-uptake of dimethylamine (DMA) and ammonia (NH_3) by sulfuric
377 acid particles at 50% RH led to particle-phase dimethylaminium (DMAH^+) to
378 ammonium (NH_4^+) molar ratio up to four times that of gas-phase DMA to ammonia
379 molar ratio (0.1 and 0.5), suggesting the displacement of NH_4^+ by DMA during the
380 uptake process (Sauerwein and Chan, 2017). In this work, the ambient RH and acidic
381 particles containing abundant sulfate and nitrate were similar to the experimental
382 conditions used in Sauerwein and Chan (2017). In summer 8% of amine-containing
383 particles contained NH_4^+ , while 25% of ammonium-containing particles contained
384 amines (Figure 7). Although the gas-phase concentrations of amines and NH_3 are not
385 quantified, higher abundance of amines in ammonium-containing particles than that of
386 ammonium in amine-containing particles suggests a possible ammonium–amine
387 exchange reactions in acidic particles in summer.

388 As strong bases, the presence of amines could have an impact on the particle
389 acidity. After including amines along with the ammonium in the relative acidity ratio
390 calculation, the new R_a' values (redefined as the ratio of the sum of the sulfate and
391 nitrate peak areas to the sum of the ammonium and amine peak areas) decrease to 11
392 ± 4 and 10 ± 2 in summer and winter, respectively, which are 30 and 3 times lower
393 than R_a values. R_a' showed no obvious seasonal change of particle acidity, which
394 suggests that amines could be a buffer for the particle acidity of ammonium-poor
395 particles, implying that it is reasonable to consider amines to calculate particle acidity
396 and actual pH.

397 **4 Summary and Conclusions**

398 Amine-containing particles were investigated using a single particle aerosol mass

399 spectrometer from 18 July to 1 August 2014, and from 27 January to 8 February 2015
400 in Heshan, China. Amine-containing particles accounted for 11.1 % and 9.4 % of the
401 total detected single particles in summer and winter, respectively; both seasons were
402 dominated by amine marker of $^{74}(\text{C}_2\text{H}_5)_2\text{NH}_2^+$ in 90% and 86% of amine-containing
403 particles in summer and winter, respectively. Amine markers of $^{59}(\text{CH}_3)_3\text{N}^+$ and
404 $^{86}(\text{C}_2\text{H}_5)_2\text{NCH}_2^+$ were detected in 4.5% and 5.5% of amine-containing particles in
405 summer, while their percentages both increased two times in winter. The amine
406 particles contained $^{74}(\text{C}_2\text{H}_5)_2\text{NH}_2^+$ and $^{86}(\text{C}_2\text{H}_5)_2\text{NCH}_2^+$ both exhibited similar
407 variation pattern with total amine-containing particles suggesting a similar emission
408 source of $^{74}(\text{C}_2\text{H}_5)_2\text{NH}_2^+$ and $^{86}(\text{C}_2\text{H}_5)_2\text{NCH}_2^+$, while the $^{59}(\text{CH}_3)_3\text{N}^+$ -containing
409 particles showed different temporal trends, and two sudden increase episodes of
410 $^{59}(\text{CH}_3)_3\text{N}^+$ in summer was possibly due to the emission sources of trimethylamine.
411 Although the increase of amine-containing particle counts mostly occurred at night,
412 no obvious correlations between amine-containing particles and RH were found in
413 summer ($r^2=0.33$) and winter ($r^2=0.0003$). More than 90% of amine-containing
414 particles contained strong signals of sulfate throughout the sampling period, while 43%
415 and 69% of amine particles contained nitrate in summer in winter. Only 8% of amine
416 particles contained ammonium in summer, while the percentage increased
417 dramatically to 54% in winter. Due to the lower percentage of total
418 ammonium-containing particles in summer (3.6%) than it in winter (32.6%), the
419 relatively ammonium-poor state of amine-containing particles in summer may be due
420 to the lower abundance of ammonia/ammonium in gas and particle phase. Besides, 8%
421 of amine-containing particles contained ammonium while 25% of
422 ammonium-containing particles contained amines in summer, suggesting a possible
423 contribution of ammonium–amine exchange reactions to the low abundance of
424 ammonium in amine-containing particles at high ambient RH (72 ± 13 %) in summer.
425 In addition, the presence of aminium salts affects the water activities and osmotic
426 coefficients of aqueous solutions, which may influence the calculation of pH using
427 aerosol thermodynamic models (Sauerwein et al., 2015). Furthermore, it should be
428 noted that the measured pH of bulk ambient aerosols may not be representative of the

429 actual single particle acidity. As pointed out in Pratt et al. (2009) and in this work, the
430 mixing state of aerosols should be considered in order to comprehensively estimate
431 the aerosol pH. Several recent studies have reported a ‘missing’ source of sulfate
432 produced from the oxidation of SO₂ by NO₂ during haze episodes with high ambient
433 relative humidity in northern China, and the neutralization of particulate ammonium is
434 a key factor in this formation mechanism (Cheng et al., 2016; Wang et al., 2016). Our
435 study reveals that amines have a potential influence on particle acidity, which could
436 also impact this sulfate formation process during haze episodes. In order to discuss the
437 potential role of amines in this sulfate formation pathway, real-time concentrations of
438 amines, ammonium, sulfate, nitrate, and their precursors must be available. The
439 results of this study suggest that amine chemistry involving particle acidity and
440 mixing state with sulfate, nitrate and ammonium may have an important role in the
441 aging process of particles in regions with high concentration of amines.

442

443

444 **Author contributions:** Chunlei Cheng and Mei Li designed the experiments. Tao
445 Zhang, Yubo Ou and Duohong Chen carried them out. Chunlei Cheng prepared the
446 manuscript with contributions from all co-authors.

447

448 **Competing interests:** Bo Huang and Zhong Fu are both employees at Guangzhou
449 Hexin Analytical Instrument Limited Company.

450

451 **Acknowledgements:** This work was financially supported by the NSFC of Guangdong
452 Province (Grant Nos. 2017A030310180, 2015A030313339), National Natural Science
453 Foundation of China (Grant No.21607056), National Key Technology R&D Program
454 (Grant No. 2014BAC21B01), Guangdong Province Public Interest Research and
455 Capacity Building Special Fund (Grant No. 2014B020216005), the Guangdong
456 Applied Science and Technology Research and Development (Grant No.
457 2015B020236003), Fundamental Research Funds for the Central Universities (Grant
458 No. 21617455), National research program for key issues in air pollution control

459 (Grant No. DQGG0107), National Key Research and Development Program of China
460 (Grant No. 2016YFC0208503), and Pearl River Nova Program of Guangzhou (No.
461 201506010013). Chak K. Chan would like to acknowledge funding support from the
462 General Fund of National Natural Science Foundation of China (Grant No. 41675117).
463 The authors acknowledge sampling support from the Guangdong Atmospheric
464 Supersite. Helpful comments and revisions from Anthony S. Wexler, Hang Su and
465 Misha I.S. Boehm are acknowledged as well.

466 **References**

- 467 Angelino, S., Suess, D. T., and Prather, K. A.: Formation of aerosol particles from
468 reactions of secondary and tertiary alkylamines: Characterization by aerosol
469 time-of-flight mass spectrometry, *Environmental Science & Technology*, 35,
470 3130-3138, 10.1021/es0015444, 2001.
- 471 Berndt, T., Stratmann, F., Sipila, M., Vanhanen, J., Petaja, T., Mikkila, J., Gruner, A.,
472 Spindler, G., Mauldin, R. L., Curtius, J., Kulmala, M., and Heintzenberg, J.:
473 Laboratory study on new particle formation from the reaction OH + SO₂:
474 influence of experimental conditions, H₂O vapour, NH₃ and the amine
475 tert-butylamine on the overall process, *Atmospheric Chemistry and Physics*, 10,
476 7101-7116, 10.5194/acp-10-7101-2010, 2010.
- 477 Bzdek, B., Ridge, D., and Johnston, M.: Amine exchange into ammonium bisulfate
478 and ammonium nitrate nuclei, *Atmospheric Chemistry and Physics*, 10,
479 3495-3503, 2010.
- 480 Cadle, S. H., and Mulawa, P. A.: Low-molecular-weight aliphatic amines in exhaust
481 from catalyst-equipped cars, *Environmental science & technology*, 14, 718-723,
482 1980.
- 483 Calderon, S. M., Poor, N. D., and Campbell, S. W.: Estimation of the particle and gas
484 scavenging contributions to wet deposition of organic nitrogen, *Atmospheric*
485 *Environment*, 41, 4281-4290, 10.1016/j.atmosenv.2006.06.067, 2007.
- 486 Chan, L. P., and Chan, C. K.: Role of the Aerosol Phase State in Ammonia/Amines
487 Exchange Reactions, *Environmental Science & Technology*, 47, 5755-5762,
488 10.1021/es4004685, 2013.
- 489 Cheng, C., Li, M., Chan, C. K., Tong, H., Chen, C., Chen, D., Wu, D., Li, L., Wu, C.,
490 Cheng, P., Gao, W., Huang, Z., Li, X., Zhang, Z., Fu, Z., Bi, Y., and Zhou, Z.:
491 Mixing state of oxalic acid containing particles in the rural area of Pearl River
492 Delta, China: implications for the formation mechanism of oxalic acid,
493 *Atmospheric Chemistry and Physics*, 17, 9519-9533, 10.5194/acp-17-9519-2017,
494 2017.
- 495 Cheng, Y., Zheng, G., Wei, C., Mu, Q., Zheng, B., Wang, Z., Gao, M., Zhang, Q., He,

496 K., Carmichael, G., Pöschl, U., and Su, H.: Reactive nitrogen chemistry in
497 aerosol water as a source of sulfate during haze events in China, *Science*
498 *Advances*, 2, 10.1126/sciadv.1601530, 2016.

499 Chu, Y., and Chan, C. K.: Reactive Uptake of Dimethylamine by Ammonium Sulfate
500 and Ammonium Sulfate–Sucrose Mixed Particles, *The Journal of Physical*
501 *Chemistry A*, 121, 206-215, 10.1021/acs.jpca.6b10692, 2016.

502 Chu, Y., and Chan, C. K.: Role of oleic acid coating in the heterogeneous uptake of
503 dimethylamine by ammonium sulfate particles, *Aerosol Science and Technology*,
504 51, 988-997, 10.1080/02786826.2017.1323072, 2017.

505 Chu, Y. X., Sauerwein, M., and Chan, C. K.: Hygroscopic and phase transition
506 properties of alkyl aminium sulfates at low relative humidities, *Phys Chem Chem*
507 *Phys*, 17, 19789-19796, 10.1039/c5cp02404h, 2015.

508 Day, D. A., Takahama, S., Gilardoni, S., and Russell, L. M.: Organic composition of
509 single and submicron particles in different regions of western North America and
510 the eastern Pacific during INTEX-B 2006, *Atmospheric Chemistry and Physics*,
511 9, 5433-5446, 2009.

512 Denkenberger, K. A., Moffet, R. C., Holecek, J. C., Rebotier, T. P., and Prather, K. A.:
513 Real-time, single-particle measurements of oligomers in aged ambient aerosol
514 particles, *Environmental Science & Technology*, 41, 5439-5446,
515 10.1021/es070329l, 2007.

516 Facchini, M. C., Decesari, S., Rinaldi, M., Carbone, C., Finessi, E., Mircea, M., Fuzzi,
517 S., Moretti, F., Tagliavini, E., Ceburnis, D., and O'Dowd, C. D.: Important
518 Source of Marine Secondary Organic Aerosol from Biogenic Amines,
519 *Environmental Science & Technology*, 42, 9116-9121, 10.1021/es8018385, 2008.

520 Gaston, C. J., Furutani, H., Guazzotti, S. A., Coffee, K. R., Bates, T. S., Quinn, P. K.,
521 Aluwihare, L. I., Mitchell, B. G., and Prather, K. A.: Unique ocean - derived
522 particles serve as a proxy for changes in ocean chemistry, *Journal of Geophysical*
523 *Research: Atmospheres* (1984–2012), 116, 10.1029/2010JD015289, 2011.

524 Gaston, C. J., Quinn, P. K., Bates, T. S., Gilman, J. B., Bon, D. M., Kuster, W. C., and
525 Prather, K. A.: The impact of shipping, agricultural, and urban emissions on
526 single particle chemistry observed aboard the R/V Atlantis during CalNex,
527 *Journal of Geophysical Research-Atmospheres*, 118, 5003-5017,
528 10.1002/jgrd.50427, 2013.

529 Ge, X. L., Wexler, A. S., and Clegg, S. L.: Atmospheric amines - Part I. A review,
530 *Atmospheric Environment*, 45, 524-546, DOI 10.1016/j.atmosenv.2010.10.012,
531 2011a.

532 Ge, X. L., Wexler, A. S., and Clegg, S. L.: Atmospheric amines - Part II.
533 Thermodynamic properties and gas/particle partitioning, *Atmospheric*
534 *Environment*, 45, 561-577, 10.1016/j.atmosenv.2010.10.013, 2011b.

535 Gilardoni, S., Liu, S., Takahama, S., Russell, L. M., Allan, J. D., Steinbrecher, R.,
536 Jimenez, J. L., De Carlo, P. F., Dunlea, E. J., and Baumgardner, D.:
537 Characterization of organic ambient aerosol during MIRAGE 2006 on three
538 platforms, *Atmospheric Chemistry and Physics*, 9, 5417-5432, 2009.

539 Glagolenko, S., and Phares, D. J.: Single-particle analysis of ultrafine aerosol in

540 College Station, Texas, *Journal of Geophysical Research-Atmospheres*, 109,
541 10.1029/2004jd004621, 2004.

542 Gross, D. S., Galli, M. E., Silva, P. J., and Prather, K. A.: Relative sensitivity factors
543 for alkali metal and ammonium cations in single particle aerosol time-of-flight
544 mass spectra, *Anal. Chem.*, 72, 416-422, Doi 10.1021/Ac990434g, 2000.

545 Guazzotti, S. A., Whiteaker, J. R., Suess, D., Coffee, K. R., and Prather, K. A.:
546 Real-time measurements of the chemical composition of size-resolved particles
547 during a Santa Ana wind episode, California USA, *Atmospheric Environment*, 35,
548 3229-3240, 2001.

549 Healy, R., Sciare, J., Poulain, L., Kamili, K., Merkel, M., Müller, T., Wiedensohler, A.,
550 Eckhardt, S., Stohl, A., and Sarda-Estève, R.: Sources and mixing state of
551 size-resolved elemental carbon particles in a European megacity: Paris,
552 *Atmospheric Chemistry and Physics*, 12, 1681-1700, 2012.

553 Healy, R. M., Evans, G. J., Murphy, M., Sierau, B., Arndt, J., McGillicuddy, E.,
554 O'Connor, I. P., Sodeau, J. R., and Wenger, J. C.: Single-particle speciation of
555 alkylamines in ambient aerosol at five European sites, *Analytical and*
556 *Bioanalytical Chemistry*, 407, 5899-5909, 10.1007/s00216-014-8092-1, 2015.

557 Huang, Y., Chen, H., Wang, L., Yang, X., and Chen, J.: Single particle analysis of
558 amines in ambient aerosol in Shanghai, *Environmental Chemistry*, 9, 202-210,
559 10.1071/EN11145, 2012.

560 Huang, Y., Li, L., Li, J., Wang, X., Chen, H., Chen, J., Yang, X., Gross, D. S., Wang,
561 H., Qiao, L., and Chen, C.: A case study of the highly time-resolved evolution of
562 aerosol chemical and optical properties in urban Shanghai, China, *Atmospheric*
563 *Chemistry and Physics*, 13, 3931-3944, 10.5194/acp-13-3931-2013, 2013.

564 Jeong, C. H., McGuire, M. L., Godri, K. J., Slowik, J. G., Rehbein, P. J. G., and Evans,
565 G. J.: Quantification of aerosol chemical composition using continuous single
566 particle measurements, *Atmospheric Chemistry and Physics*, 11, 7027-7044,
567 10.5194/acp-11-7027-2011, 2011.

568 Kurten, T., Loukonen, V., Vehkamäki, H., and Kulmala, M.: Amines are likely to
569 enhance neutral and ion-induced sulfuric acid-water nucleation in the atmosphere
570 more effectively than ammonia, *Atmospheric Chemistry and Physics*, 8,
571 4095-4103, 2008.

572 Lee, D., and Wexler, A. S.: Atmospheric amines - Part III: Photochemistry and toxicity,
573 *Atmospheric Environment*, 71, 95-103, DOI 10.1016/j.atmosenv.2013.01.058,
574 2013.

575 Li, L., Huang, Z. X., Dong, J. G., Li, M., Gao, W., Nian, H. Q., Fu, Z., Zhang, G. H.,
576 Bi, X. H., Cheng, P., and Zhou, Z.: Real time bipolar time-of-flight mass
577 spectrometer for analyzing single aerosol particles, *Int J Mass Spectrom*, 303,
578 118-124, 10.1016/j.ijms.2011.01.017, 2011.

579 Liu, S., Takahama, S., Russell, L. M., Gilardoni, S., and Baumgardner, D.:
580 Oxygenated organic functional groups and their sources in single and submicron
581 organic particles in MILAGRO 2006 campaign, *Atmospheric Chemistry and*
582 *Physics*, 9, 6849-6863, 2009.

583 Liu, Y., Han, C., Liu, C., Ma, J., Ma, Q., and He, H.: Differences in the reactivity of

584 ammonium salts with methylamine, *Atmospheric Chemistry and Physics*, 12,
585 4855-4865, 2012.

586 Lloyd, J. A., Heaton, K. J., and Johnston, M. V.: Reactive uptake of trimethylamine
587 into ammonium nitrate particles, *The Journal of Physical Chemistry A*, 113,
588 4840-4843, 10.1021/jp900634d, 2009.

589 Malloy, Q. G. J., Li, Q., Warren, B., Cocker Iii, D. R., Erupe, M. E., and Silva, P. J.:
590 Secondary organic aerosol formation from primary aliphatic amines with NO₃
591 radical, *Atmos. Chem. Phys.*, 9, 2051-2060, 10.5194/acp-9-2051-2009, 2009.

592 Moffet, R. C., de Foy, B., Molina, L. T., Molina, M. J., and Prather, K. A.:
593 Measurement of ambient aerosols in northern Mexico City by single particle
594 mass spectrometry, *Atmospheric Chemistry and Physics*, 8, 4499-4516,
595 10.5194/acp-8-4499-2008, 2008.

596 Murphy, S. M., Sorooshian, A., Kroll, J. H., Ng, N. L., Chhabra, P., Tong, C., Surratt,
597 J. D., Knipping, E., Flagan, R. C., and Seinfeld, J. H.: Secondary aerosol
598 formation from atmospheric reactions of aliphatic amines, *Atmospheric
599 Chemistry and Physics*, 7, 2313-2337, 2007.

600 Ngwabie, N. M., Schade, G. W., Custer, T. G., Linke, S., and Hinz, T.: Volatile organic
601 compound emission and other trace gases from selected animal buildings,
602 *Landbauforsch Volk*, 57, 273-284, 2007.

603 Noble, C. A., and Prather, K. A.: Real-time measurement of correlated size and
604 composition profiles of individual atmospheric aerosol particles, *Environmental
605 science & technology*, 30, 2667-2680, 1996.

606 Phares, D. J., Rhoads, K. P., Johnston, M. V., and Wexler, A. S.: Size-resolved
607 ultrafine particle composition analysis - 2. Houston, *Journal of Geophysical
608 Research-Atmospheres*, 108, 10.1029/2001jd001212, 2003.

609 Place, P. F., Ziemba, L. D., and Griffin, R. J.: Observations of nucleation-mode
610 particle events and size distributions at a rural New England site, *Atmospheric
611 Environment*, 44, 88-94, 10.1016/j.atmosenv.2009.09.030, 2010.

612 Prather, K. A., Nordmeyer, T., and Salt, K.: Real-time characterization of individual
613 aerosol particles using time-of-flight mass spectrometry, *Anal. Chem.*, 66,
614 1403-1407, 1994.

615 Pratt, K. A., Hatch, L. E., and Prather, K. A.: Seasonal Volatility Dependence of
616 Ambient Particle Phase Amines, *Environmental Science & Technology*, 43,
617 5276-5281, 10.1021/es803189n, 2009.

618 Pratt, K. A., and Prather, K. A.: Mass spectrometry of atmospheric aerosols—Recent
619 developments and applications. Part II: On - line mass spectrometry techniques,
620 *Mass Spectrom Rev*, 31, 17-48, 2012.

621 Qin, X. Y., Pratt, K. A., Shields, L. G., Toner, S. M., and Prather, K. A.: Seasonal
622 comparisons of single-particle chemical mixing state in Riverside, CA,
623 *Atmospheric Environment*, 59, 587-596, 10.1016/j.atmosenv.2012.05.032, 2012.

624 Qiu, C., Wang, L., Lal, V., Khalizov, A. F., and Zhang, R.: Heterogeneous reactions of
625 alkylamines with ammonium sulfate and ammonium bisulfate, *Environmental
626 science & technology*, 45, 4748-4755, 2011.

627 Rappert, S., and Muller, R.: Odor compounds in waste gas emissions from agricultural

628 operations and food industries, *Waste Manage*, 25, 887-907,
629 10.1016/j.wasman.2005.07.008, 2005.

630 Rehbein, P. J. G., Jeong, C. H., McGuire, M. L., Yao, X. H., Corbin, J. C., and Evans,
631 G. J.: Cloud and Fog Processing Enhanced Gas-to-Particle Partitioning of
632 Trimethylamine, *Environmental Science & Technology*, 45, 4346-4352,
633 10.1021/es1042113, 2011.

634 Rogge, W. F., Hildemann, L. M., Mazurek, M. A., and Cass, G. R.: Sources of Fine
635 Organic Aerosol .6. Cigarette-Smoke in the Urban Atmosphere, *Environmental
636 Science & Technology*, 28, 1375-1388, 10.1021/Es00056a030, 1994.

637 Russell, L. M., Takahama, S., Liu, S., Hawkins, L. N., Covert, D. S., Quinn, P. K., and
638 Bates, T. S.: Oxygenated fraction and mass of organic aerosol from direct
639 emission and atmospheric processing measured on the R/V Ronald Brown during
640 TEXAQS/GoMACCS 2006, *Journal of Geophysical Research-Atmospheres*, 114,
641 10.1029/2008jd011275, 2009.

642 Sauerwein, M., Clegg, S. L., and Chan, C. K.: Water Activities and Osmotic
643 Coefficients of Aqueous Solutions of Five Alkylammonium Sulfates and Their
644 Mixtures with H₂SO₄ at 25(o)C, *Aerosol Science and Technology*, 49, 566-579,
645 10.1080/02786826.2015.1043045, 2015.

646 Sauerwein, M., and Chan, C. K.: Heterogeneous uptake of ammonia and
647 dimethylamine into sulfuric and oxalic acid particles, *Atmos. Chem. Phys.*, 17,
648 6323-6339, 10.5194/acp-17-6323-2017, 2017.

649 Silva, P. J., Erupe, M. E., Price, D., Elias, J., Malloy, Q. G. J., Li, Q., Warren, B., and
650 Cocker, D. R.: Trimethylamine as precursor to secondary organic aerosol
651 formation via nitrate radical reaction in the atmosphere, *Environmental Science
652 & Technology*, 42, 4689-4696, Doi 10.1021/Es703016v, 2008.

653 Sorooshian, A., Ng, N. L., Chan, A. W. H., Feingold, G., Flagan, R. C., and Seinfeld, J.
654 H.: Particulate organic acids and overall water-soluble aerosol composition
655 measurements from the 2006 Gulf of Mexico Atmospheric Composition and
656 Climate Study (GoMACCS), *Journal of Geophysical Research-Atmospheres*,
657 112, 10.1029/2007jd008537, 2007.

658 Sorooshian, A., Murphy, S. N., Hersey, S., Gates, H., Padro, L. T., Nenes, A., Brechtel,
659 F. J., Jonsson, H., Flagan, R. C., and Seinfeld, J. H.: Comprehensive airborne
660 characterization of aerosol from a major bovine source, *Atmospheric Chemistry
661 and Physics*, 8, 5489-5520, 2008.

662 Wang, G., Zhang, R., Gomez, M. E., Yang, L., Levy Zamora, M., Hu, M., Lin, Y.,
663 Peng, J., Guo, S., Meng, J., Li, J., Cheng, C., Hu, T., Ren, Y., Wang, Y., Gao, J.,
664 Cao, J., An, Z., Zhou, W., Li, G., Wang, J., Tian, P., Marrero-Ortiz, W., Secretst, J.,
665 Du, Z., Zheng, J., Shang, D., Zeng, L., Shao, M., Wang, W., Huang, Y., Wang, Y.,
666 Zhu, Y., Li, Y., Hu, J., Pan, B., Cai, L., Cheng, Y., Ji, Y., Zhang, F., Rosenfeld, D.,
667 Liss, P. S., Duce, R. A., Kolb, C. E., and Molina, M. J.: Persistent sulfate
668 formation from London Fog to Chinese haze, *Proceedings of the National
669 Academy of Sciences*, 113, 13630-13635, 10.1073/pnas.1616540113, 2016.

670 Wang, L., Khalizov, A. F., Zheng, J., Xu, W., Ma, Y., Lal, V., and Zhang, R. Y.:
671 Atmospheric nanoparticles formed from heterogeneous reactions of organics, *Nat*

672 Geosci, 3, 238-242, 10.1038/NGEO778, 2010.
673 Wang, Y. Q.: MeteoInfo: GIS software for meteorological data visualization and
674 analysis, Meteorol Appl, 21, 360-368, 10.1002/met.1345, 2014.
675 Williams, B. J., Goldstein, A. H., Kreisberg, N. M., Hering, S. V., Worsnop, D. R.,
676 Ulbrich, I. M., Docherty, K. S., and Jimenez, J. L.: Major components of
677 atmospheric organic aerosol in southern California as determined by hourly
678 measurements of source marker compounds, Atmospheric Chemistry and Physics,
679 10, 11577-11603, 10.5194/acp-10-11577-2010, 2010.
680 Wu, C., Wu, D., and Yu, J. Z.: Quantifying black carbon light absorption enhancement
681 with a novel statistical approach, Atmospheric Chemistry and Physics, 18,
682 289-309, 10.5194/acp-18-289-2018, 2018.
683 Wu, C., and Yu, J. Z.: Evaluation of linear regression techniques for atmospheric
684 applications: the importance of appropriate weighting, Atmos Meas Tech, 11,
685 1233-1250, 10.5194/amt-11-1233-2018, 2018.
686 Zauscher, M. D., Wang, Y., Moore, M. J. K., Gaston, C. J., and Prather, K. A.: Air
687 Quality Impact and Physicochemical Aging of Biomass Burning Aerosols during
688 the 2007 San Diego Wildfires, Environmental Science & Technology, 47,
689 7633-7643, 10.1021/es4004137, 2013.
690 Zhang, G., Bi, X., Chan, L. Y., Li, L., Wang, X., Feng, J., Sheng, G., Fu, J., Li, M.,
691 and Zhou, Z.: Enhanced trimethylamine-containing particles during fog events
692 detected by single particle aerosol mass spectrometry in urban Guangzhou, China,
693 Atmospheric Environment, 55, 121-126, 2012.
694
695
696
697
698
699
700
701
702
703
704
705
706
707
708
709
710
711
712
713
714
715

716 **Tables and Figures**

717 **Table list:**

718 Table 1. Marker ions chosen for the amine-containing particles

719

720 Table 2. Seasonal distributions of amine-containing particles and three major amine
721 markers in summer and winter in the PRD, China.

722

723 Table 3. The abundances of ammonium-, nitrate- and sulfate-containing amine
724 particles in total amine-containing particles.

725 **Figure captions:**

726 Figure 1. Spatial distributions of amine-containing particle counts associated with
727 backward trajectories (48 hour) of air masses at 500m levels above the ground during
728 the sampling period: (a) summer (from July 18 to August 1, 2014), (b) winter (from
729 January 27 to February 8, 2015).

730

731 Figure 2. Temporal variations of relative humidity (RH), temperature (T), total
732 amine-containing particles, and three major marker ions-containing amine particles
733 ($^{59}(\text{CH}_3)_3\text{N}^+$, $^{74}(\text{C}_2\text{H}_5)_2\text{NH}_2^+$, $^{86}(\text{C}_2\text{H}_5)_2\text{NCH}_2^+$) in Heshan, China during sampling
734 periods.

735

736 Figure 3. Diurnal variations of amine-containing particle counts in summer and winter
737 in Heshan.

738

739 Figure 4. Average ion mass spectra of amine-containing particles in summer and
740 winter. The color bars represent each peak area corresponding to a specific ion in
741 individual particles.

742

743 Figure 5. Unscaled size-resolved number distributions of total amine-containing
744 particles and amine particles containing three marker ions of $^{59}(\text{CH}_3)_3\text{N}^+$,
745 $^{74}(\text{C}_2\text{H}_5)_2\text{NH}_2^+$, and $^{86}(\text{C}_2\text{H}_5)_2\text{NCH}_2^+$ in summer and winter in Heshan.

746

747 Figure 6. Mass spectra of total ammonium-containing (NH_4^+ -containing) particles in
748 summer and winter. The color bars represent each peak area corresponding to a
749 specific fraction in individual particles.

750

751 Figure 7. Temporal variations of total amine-containing particles, total
752 ammonium-containing particles, and particles containing both ammonium and amine
753 (NH_4^+ -amine) during sampling period in Heshan.

754

755 Figure 8. Temporal variations of the peak areas of amines, ammonium, sulfate and
756 nitrate in amine-containing particles during summer and winter. The relative acidity

757 ratio (R_a), which was calculated as the ratio of the total sulfate and nitrate peak areas
758 to the ammonium peak area, is plotted as $\log(R_a)$.

759

760

761

762

763

764

765

766

767

768

769

770

771

772

773

774

775

776

777

778

779

780

781

782

783

784

785

786

787

788

789

790

791

792

793

794

795

796

797

798

799

800

801 **Tables:**

802

Table 1. Marker ions chosen for the amine-containing particles

Marker ion	Alkylamine assignment
$^{59}(\text{CH}_3)_3\text{N}^+$	Trimethylamine (TMA) ^a
$^{74}(\text{C}_2\text{H}_5)_2\text{NH}_2^+$	Diethylamine (DEA) ^b
$^{86}(\text{C}_2\text{H}_5)_2\text{NCH}_2^+$	DEA, TEA, DPA ^c
$^{101}(\text{C}_2\text{H}_5)_3\text{N}^+$	Triethylamine (TEA) ^d
$^{102}(\text{C}_3\text{H}_7)_2\text{NH}_2^+$	Dipropylamine (DPA) ^e
$^{143}(\text{C}_3\text{H}_7)_3\text{N}^+$	Tripropylamine (TPA) ^f

References are as follows: ^aZhang et al., 2012, Gaston et al., 2013; ^bAngelino et al., 2001; ^cHuang et al., 2012, Zauscher et al., 2013, Qin et al., 2012; ^dGaston et al., 2013; ^ePratt et al., 2009; ^fHealy et al., 2015.

803

804

805

806

807

Table 2. Seasonal distributions of amine-containing particles and three major amine markers in summer and winter in the PRD, China.

Particle type	Summer (18/7-1/8, 2014)		Winter (27/1-8/2, 2015)	
	Count	Percentage (%) ^a	Count	Percentage (%) ^a
Total Amines	57452		68026	
$^{59}(\text{CH}_3)_3\text{N}^+$	2581	4.5	6894	10
$^{74}(\text{C}_2\text{H}_5)_2\text{NH}_2^+$	51442	90	58272	86
$^{86}(\text{C}_2\text{H}_5)_2\text{NCH}_2^+$	3185	5.5	6119	9

^aThe percentage of each amine marker ion in total detected amine-containing particles.

808

809

810

811

Table 3. The abundances of ammonium-, nitrate- and sulfate-containing amine particles in total amine-containing particles.

Marker ions	Summer	Winter
$^{18}\text{NH}_4^+$	8%	54%
$^{62}\text{NO}_3^-$	43%	69%
$^{97}\text{HSO}_4^-$	91%	94%

The marker ions of $^{18}\text{NH}_4^+$, $^{62}\text{NO}_3^-$ and $^{97}\text{HSO}_4^-$ were chosen to represent ammonium, nitrate and sulfate.

812

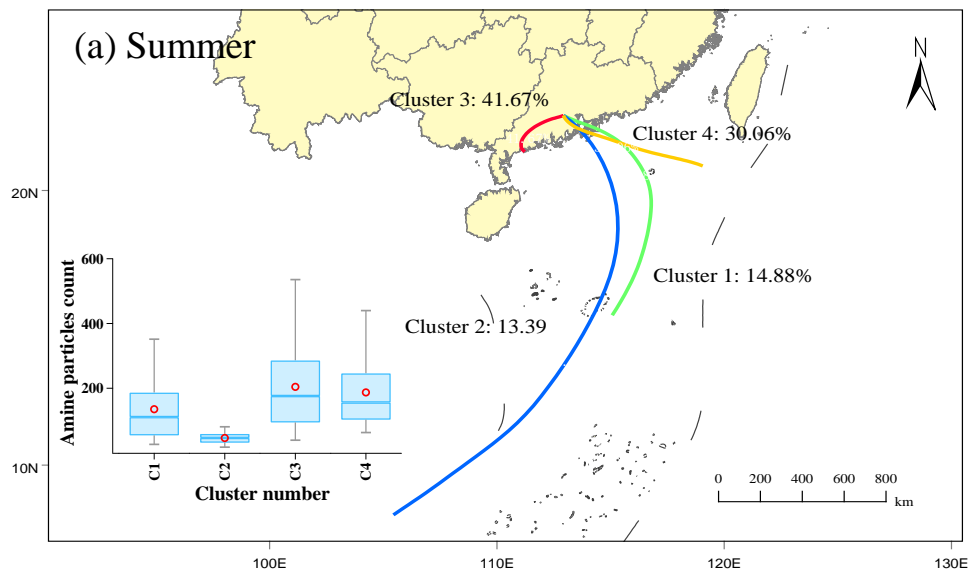
813

814

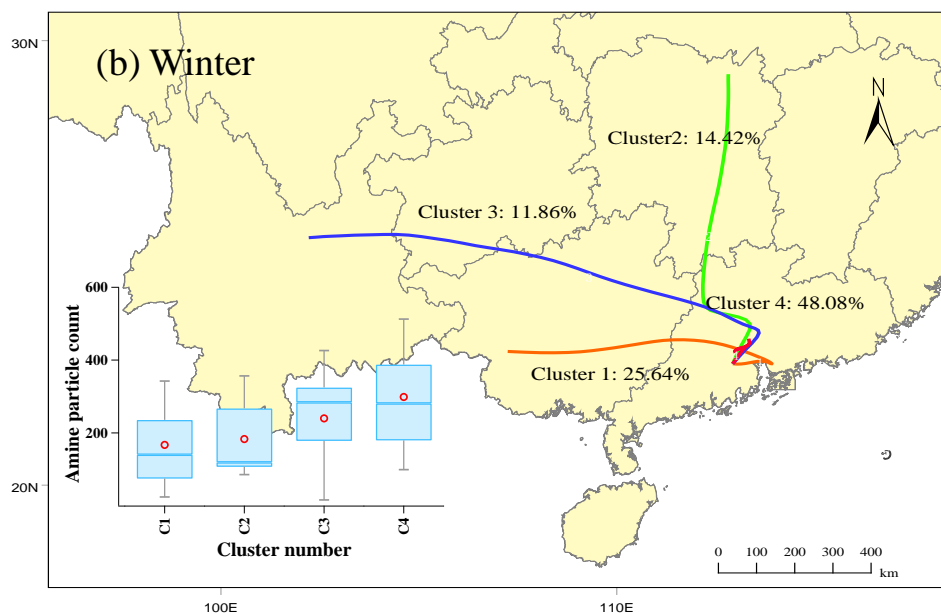
815

816 **Figures:**

817



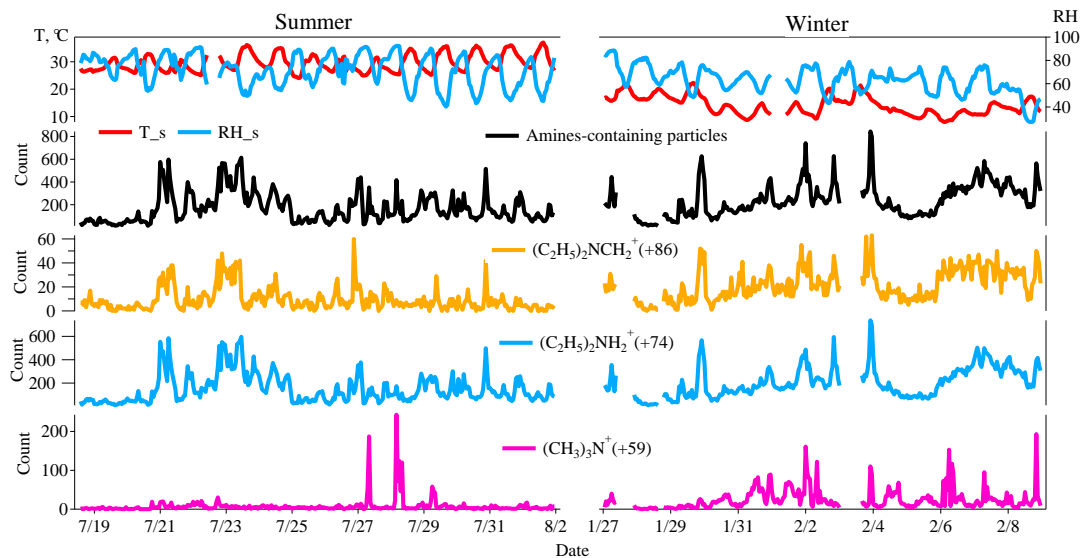
818



819

820 Figure 1. Spatial distributions of amine-containing particle counts associated with
821 backward trajectories (48 hour) of air masses at 500m levels above the ground during
822 the sampling period: (a) summer (from July 18 to August 1, 2014), (b) winter (from
823 January 27 to February 8, 2015).

824



825

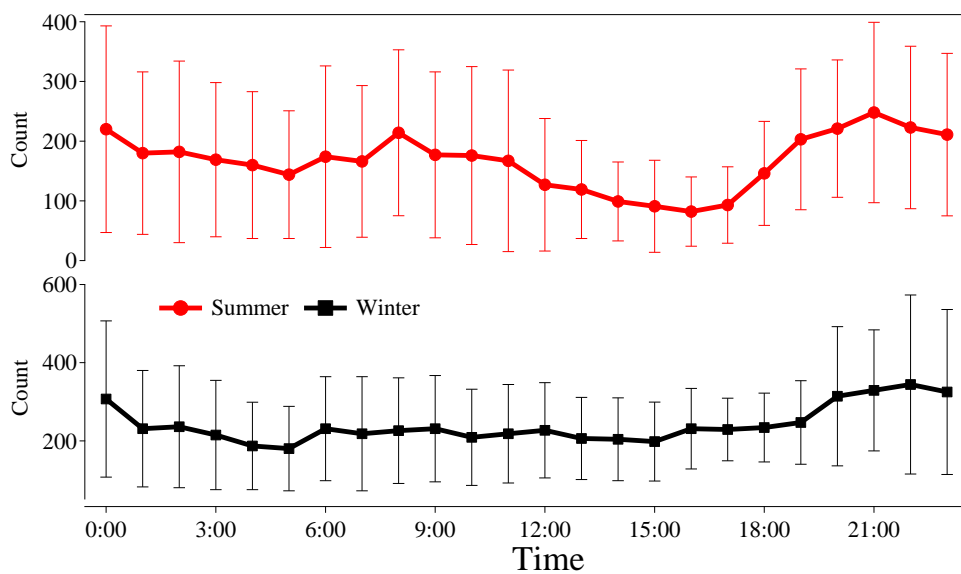
826 Figure 2. Temporal variations of relative humidity (RH), temperature (T), total
 827 amine-containing particles, and three major marker ions-containing amine particles
 828 ($^{59}\text{(CH}_3)_3\text{N}^+$, $^{74}\text{(C}_2\text{H}_5)_2\text{NH}_2^+$, $^{86}\text{(C}_2\text{H}_5)_2\text{NCH}_2^+$) in Heshan, China during sampling periods.

829

830

831

832



833

834 Figure 3. Diurnal variations of amine-containing particle counts in summer and winter
 835 in Heshan.

836

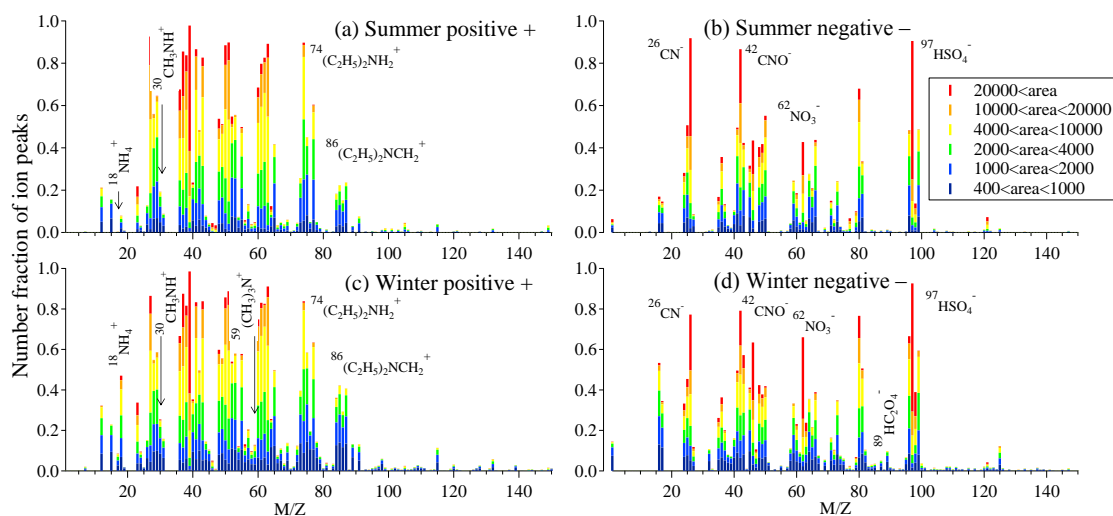
837

838

839

840

841



842

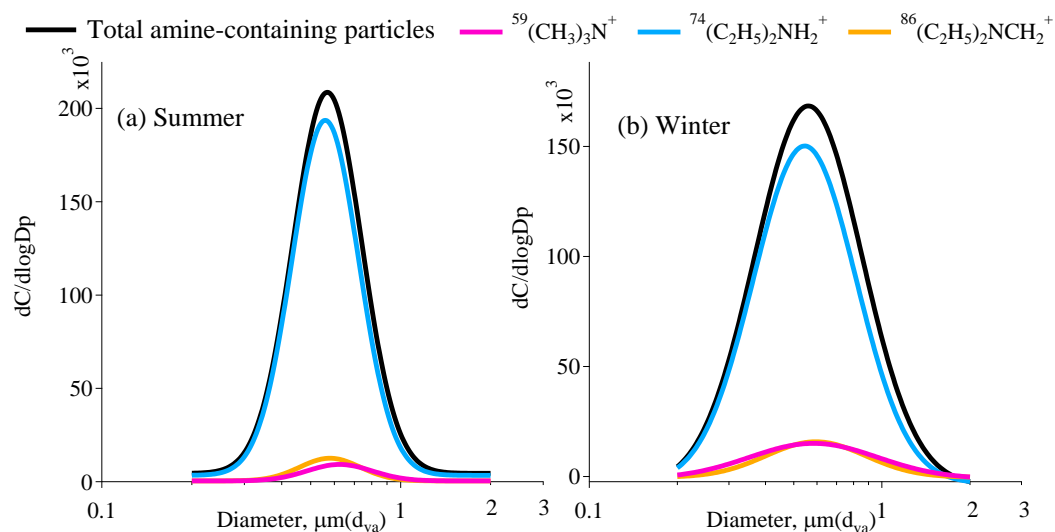
843 Figure 4. Average ion mass spectra of amine-containing particles in summer and
 844 winter. The color bars represent each peak area corresponding to a specific ion in
 845 individual particles.

846

847

848

849



850

851 Figure 5. Unscaled size-resolved number distributions of total amine-containing
 852 particles and amine particles containing three marker ions of $^{59}(\text{CH}_3)_3\text{N}^+$,
 853 $^{74}(\text{C}_2\text{H}_5)_2\text{NH}_2^+$, and $^{86}(\text{C}_2\text{H}_5)_2\text{NCH}_2^+$ in summer and winter in Heshan.

854

855

856

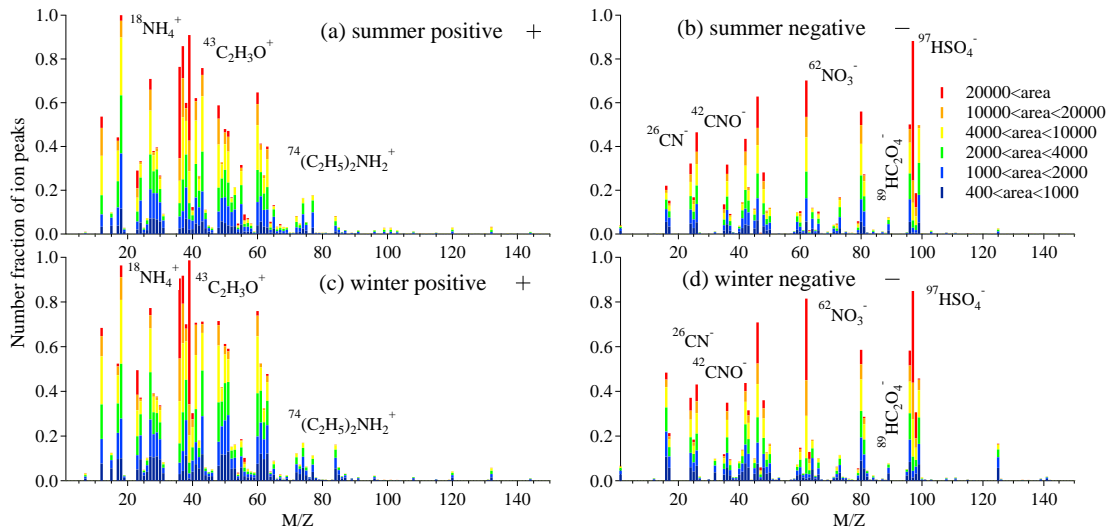
857

858

859

860

861



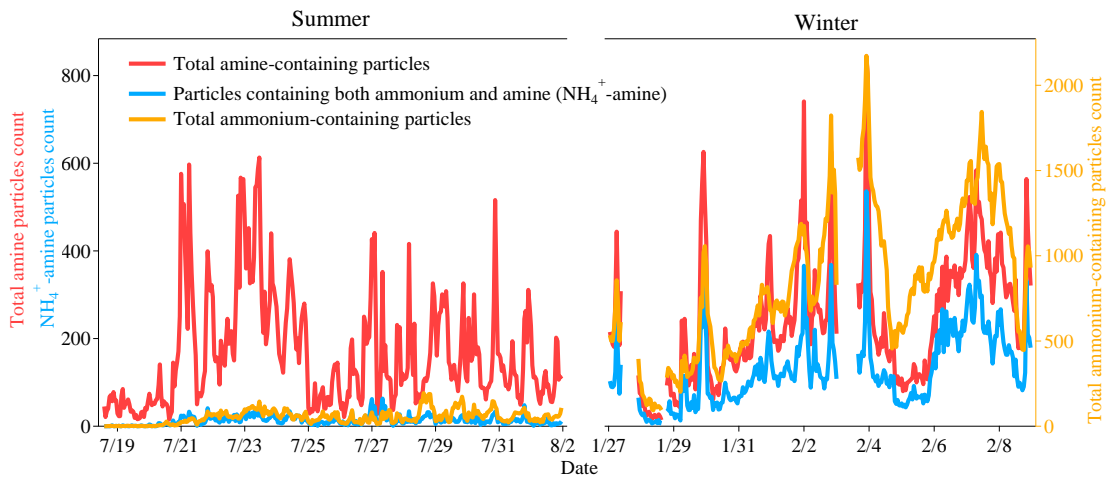
862

863 Figure 6. Mass spectra of total ammonium-containing (NH_4^+ -containing) particles in
864 summer and winter. The color bars represent each peak area corresponding to a
865 specific fraction in individual particles.

866

867

868



869

870 Figure 7. Temporal variations of total amine-containing particles, total
871 ammonium-containing particles and particles containing both ammonium and amine
872 (NH_4^+ -amine) during sampling period in Heshan.

873

874

875

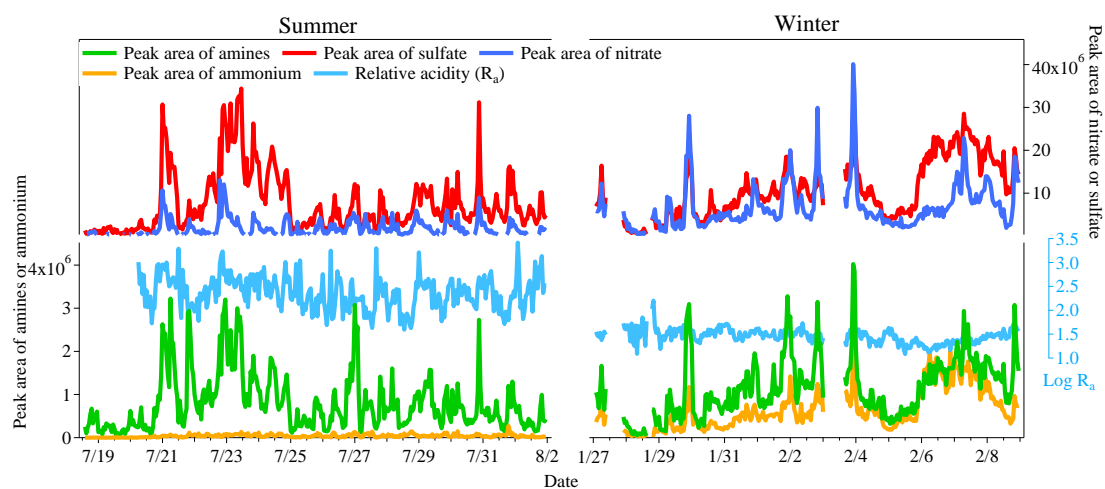
876

877

878

879

880



881

882 Figure 8. Temporal variations of the peak areas of amines, ammonium, sulfate and
883 nitrate in amine-containing particles during summer and winter. The relative acidity
884 ratio (R_a), which was calculated as the ratio of the total sulfate and nitrate peak areas
885 to the ammonium peak area, is plotted as $\log(R_a)$.

886